Received: 26 July 2019 | Revised: 29 August 2019 | Accepted: 2 September 2019

DOI: 10.1002/er.4887

TECHNICAL NOTE

WILEY INTERNATIONAL JOURNAL OF ENERGY RESEARCH

# Enhancement of hydrogen storage properties of $Ca_3CH$ antiperovskite compound with hydrogen doping

**Aysenur Gencer**[1,2] | **Gokhan Surucu**[1,3]

[1] Physics Department, Middle East Technical University, Ankara, Turkey

[2] Physics Department, Karamanoglu Mehmetbey University, Karaman, Turkey

[3] Electric and Energy Department, Ahi Evran University, Kirsehir, Turkey

**Correspondence**
Gokhan Surucu, Electric and Energy Department, Ahi Evran University, Kirsehir 40100, Turkey.
Email: g_surucu@yahoo.com

**Summary**

The doping effect of hydrogen on the $Ca_3CH_x$ ($x$ = 1, 4, 7, 9, and 10) antiperovskite compounds has been examined using density functional theory (DFT). The results of the structural optimizations show that all these compounds have negative formation energy implying the energetic stability and synthesizability. The band structures that are essential for the electronic properties have been determined along with the partial density of states (DOS) showing the metallic behavior of these compounds. In addition, the electron-density distribution has been determined, and the charge of each ion in the structures has been obtained with the Bader partial charge analysis. Moreover, the electronic stability of these compounds has been determined using the band filling theory and the number of the electrons at the Fermi level. The results of the formation enthalpy and the electronic stability investigations imply that the most stable structure is $Ca_3CH$ among the considered compounds. $Ca_3CH_{10}$ has the gravimetric storage capacity as 7.10 wt% that is the largest capacity among the considered compounds. Also, $Ca_3CH_9$ has the smallest hydrogen desorption temperature as 468.4 K among the studied compounds.

**KEYWORDS**

antiperovskite materials, electronic properties, first principle, hydrogen storage

## 1 | INTRODUCTION

The International Energy Agency investigates the world energy demand, and they have been found that the world energy demand will increase 25% between today and 2040 in the New Energy Scenario[1] because of the technology development and the population growth. Therefore, new energy sources have been investigated, and hydrogen energy is one of the potential energy sources for the future energy problem because of the high abundance of hydrogen in the earth. In the future, hydrogen economy includes production, storage, and usage of hydrogen.[2] Therefore, the storage of hydrogen is the motivation of this study.

The solid-state hydrogen storage is the most encouraging method for the hydrogen storage, and it is divided into two categories: physically bound hydrogen and chemically bound hydrogen. The physically bound hydrogen is obtained with the bonds between the hydrogen atoms and the surface of a material,[3] and the chemically bound hydrogen is obtained with the bonds between the hydrogen atoms and the material.[4,5] For the physically bound hydrogen, low temperatures are required in order to obtain a high storage capacity.[6,7] In contrast to the physically bound hydrogen, high temperatures are required to release of hydrogen for the chemically bound hydrogen.[6] High gravimetric and volumetric capacities, reversibility, good kinetics, storage, and release at

  

ambient conditions must be satisfied for an efficient hydrogen storage.[8]

In the literature, metal hydrides, complex hydrides, and carbon materials[9-24] are commonly studied materials for hydrogen storage. However, these material groups have some drawbacks such as $MgH_2$, most studied metal hydride, has low hydrogen desorption kinetics and high reactivity to air and oxygen.[25] The drawback for the complex hydrides is the nonreversibility.[26] So promising materials are still under investigation that satisfy the required conditions for a sufficient hydrogen storage. A material group has been studied extensively in the literature that is the perovskite-type hydrides having high storage capacities.[27-34] Also, effect of the dopants to the perovskite-type hydrides for the hydrogen release has been studied.[29,35] However, even perovskite-type hydrides have not been satisfied the required properties for an effective hydrogen storage material.

Perovskite materials having $ABX_3$ formula could be probable compounds for the chemically bound hydrogen storage method because of being hard and ceramic.[36] Recently, a few studies consider the perovskite materials for hydrogen storage applications.[37-39] In these studies, hydrogen atoms are doped to the perovskite materials, and their hydrogen storage characteristics have been determined. Gencer et al[37] present the study for $MgTiO_3$ and $CaTiO_3$ perovskite materials, and it has been found that $CaTiO_3H_6$ has 4.27 wt% gravimetric hydrogen storage capacity with thermodynamic and mechanical stabilities. Also, $BaScO_3$ perovskite material has been studied for the five possible crystal structures, and the hydrogen doping studies have been performed to the most stable crystal structure that is the orthorhombic phase.[38] The study by Gencer and Surucu[38] reveals that the gravimetric hydrogen storage capacity of the hydrogen-doped $BaScO_3H_{0.5}$ is 0.22 wt%. In addition, $BaYO_3$ perovskite material has been investigated, and after the hydrogen doping studies, it has been found that $BaYO_3H_3$ is thermodynamically and mechanically stable compound with 1.09 wt% gravimetric hydrogen storage capacity.[39]

Antiperovskite materials having $X_3AB$ formula are also in the group of the perovskite materials. The only difference between the antiperovskite materials and the perovskite materials is that there are two anions and one cation in the antiperovskite structure whereas there are two cations and one anion in the perovskite structure. The positions of the cation and the anion are reversed for the antiperovskite structure. So the antiperovskite materials could be a possible material group with appropriate properties for the hydrogen storage applications. The aim of this study is to examine the hydrogen storage applications of $Ca_3CH$ antiperovskite material that composes from abundant elements as Ca, C, and H.

## 2 | COMPUTATIONAL DETAILS

Density functional theory (DFT) calculations have been carried out with the Vienna Ab initio Simulation Package (VASP)[40,41] in this study. The electron-ion interaction has been considered with the projector-augmented-wave (PAW) method[42,43] with a kinetic energy cut off of 550 eV. The electron-electron interaction has been examined using the Perdew-Burke-Ernzerhof (PBE)[44] functional within the generalized gradient approximation (GGA). The $10 \times 10 \times 10$ k-points mesh has been received with

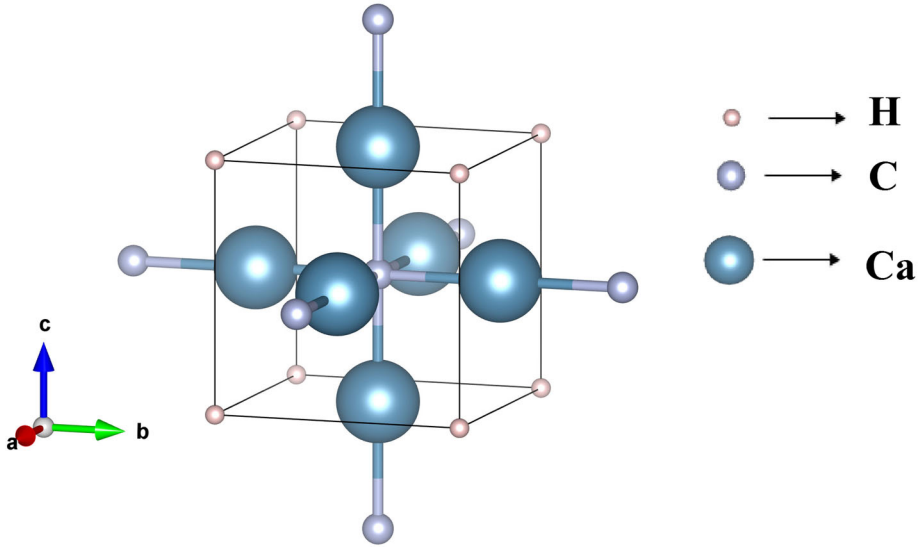


**FIGURE 1** Crystal structure for *$Ca_3CH$* [Colour figure can be viewed at wileyonlinelibrary.com]

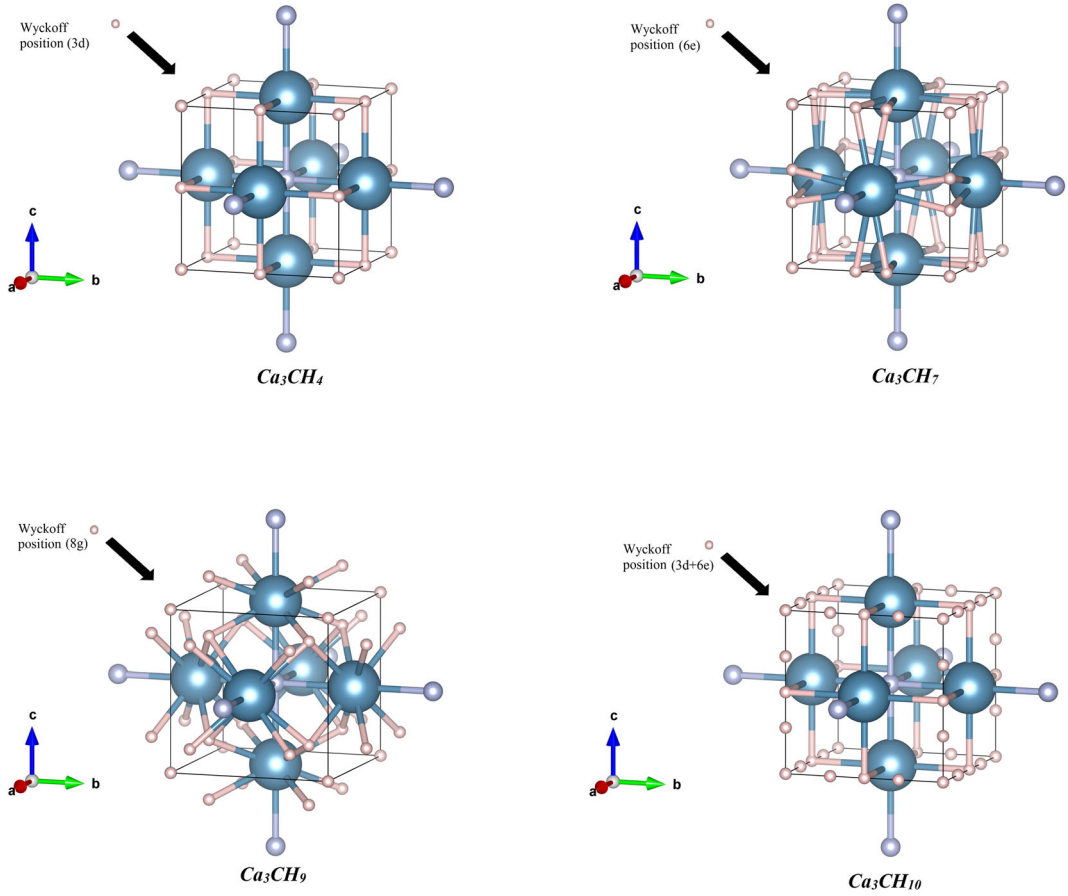


**FIGURE 2** Crystal structures for $Ca_3CH_4$, $Ca_3CH_7$, $Ca_3CH_9$, and $Ca_3CH_{10}$ [Colour figure can be viewed at wileyonlinelibrary.com]

**TABLE 1** The lattice parameter $a$, density $\rho$, formation enthalpy $\Delta E_f$, atomic positions, $W_{occ}/W_b$ ratio, number of electrons at the Fermi level, gravimetric storage capacity $C_{wt\%}$, hydrogen desorption temperature $T$ for $Ca_3CH_x$ ($x$ = 1, 4, 7, 9, and 10)

| Compound | $a$, Å | $\rho$, g/cm$^3$ | $\Delta E_f$, eV/atom | Atomic Positions | $W_{occ}/W_b$ | n | $C_{wt\%}$ | $T$, K |
|---|---|---|---|---|---|---|---|---|
| $Ca_3CH$ | 5.02 | 1.75 | −2.56 | Ca: 3c (0.000, 0.500, 0.500)<br>C: 1b (0.500, 0.500, 0.500)<br>H: 1a (0.000, 0.000, 0.000) | 1.00 | 0.42 | 0.76 | 1891 |
| $Ca_3CH_4$ | 4.92 | 1.90 | −1.60 | Ca: 3c (0.000, 0.500, 0.500)<br>C: 1b (0.500, 0.500, 0.500)<br>$H_1$: 1a (0.000, 0.000, 0.000)<br>$H_2$: 3d (0.500, 0.000, 0.000) | 0.95 | 2.15 | 2.96 | 1184 |
| $Ca_3CH_7$ | 5.04 | 1.81 | −1.11 | Ca: 3c (0.000, 0.500, 0.500)<br>C: 1b (0.500, 0.500, 0.500)<br>$H_1$:1a (0.000, 0.000, 0.000)<br>$H_2$: 6e (0.584, 0.000, 0.000) | 1.01 | 0.65 | 5.08 | 818 |
| $Ca_3CH_9$ | 5.40 | 1.49 | −0.63 | Ca: 3c (0.000, 0.500, 0.500)<br>C: 1b (0.500, 0.500, 0.500)<br>$H_1$:1a (0.000, 0.000, 0.000)<br>$H_2$: 8g (0.294, 0.294, 0.294) | 0.97 | 0.92 | 6.43 | 468 |
| $Ca_3CH_{10}$ | 5.06 | 1.83 | −0.72 | Ca: 3c (0.000, 0.500, 0.500)<br>C: 1b (0.500, 0.500, 0.500)<br>$H_1$:1a (0.000, 0.000, 0.000)<br>$H_2$: 3d (0.500, 0.000, 0.000)<br>$H_3$: 6e (0.708, 0.000, 0.000) | 0.96 | 0.72 | 7.10 | 534 |

a gamma-centered grid.[45] The structures have been optimized up to $10^{-10}$ eV per unit cell energy convergence. Also, the stresses and Hellman-Feynman forces have been minimized up to $10^{-9}$ eV/Å force convergence. VASP has been used for the Bader charge investigation, and the algorithm established by Tang et al[46] has been employed to analyze the obtained results.

## 3 | RESULTS AND DISCUSSIONS

Figure 1 shows the lattice structure for $Ca_3CH$ that belongs to the space group 221 (Pm-3m). Ca atoms are at the 3c Wyckoff positions, C atom is at the 1a Wyckoff position, and H atom is at the 1b Wyckoff position. The formation enthalpy ($\Delta E_f$) has been calculated using Equation (1), and the result implies that $Ca_3CH$ is thermodynamically stable and synthesizable. For $Ca_3CH$ compound, the obtained results could not be compared with the literature because there is no study for this compound. For hydrogen bonding studies, the possible Wyckoff positions of the space group 221 have been determined. With the hydrogen additions at the 3d, 6e, 8g, and 3d+6e Wyckoff positions,[47] $Ca_3CH_4$, $Ca_3CH_7$, $Ca_3CH_9$, and $Ca_3CH_{10}$ have been obtained as shown in Figure 2. $Ca_3CH_4$, $Ca_3CH_7$, $Ca_3CH_9$, and $Ca_3CH_{10}$ have been optimized, and the obtained lattice constants are listed in Table 1. Also, the atomic positions have been listed in Table 1. As can be concluded from Table 1, $Ca_3CH_x$ compounds are thermodynamically stable and synthesizable. The order of the stability is as follows: $Ca_3CH > Ca_3CH_4 > Ca_3CH_7 > Ca_3CH_{10} > Ca_3CH_9$.

$$\Delta E_f(Ca_3CH_x) = E_{Total}^{Ca_3CH_x} - 3.E_{Solid}^{Ca} - E_{Solid}^{C} - 3.x.E_{Solid}^{H} \quad (1)$$

The hydrogen storage properties of $Ca_3CH_x$ antiperovskite compounds have been explored and listed in Table 1. The measure of hydrogen deposited per mass of a material is defined as the gravimetric storage capacity, and in Baysal et al,[15] an equation is given to obtain this capacity. For the studied compounds, if the material has higher hydrogen atoms, the gravimetric storage capacity increases as expected. Also, the United States Department of Energy has set targets for the portable hydrogen power equipment, and the gravimetric hydrogen storage capacity target is 3.0 wt% for rechargeable equipment.[48] As can be concluded from Table 1, $Ca_3CH$ has low gravimetric capacity considering the target while the capacity increases (0.76 to 7.10 wt%) with the hydrogen doping to $Ca_3CH$ with satisfying the target. The necessary temperature to discharge the deposited hydrogen in the material is defined as the hydrogen desorption temperature, and it can be determined using Equation (2). The formation enthalpy is given as $\Delta H$ and the entropy difference of hydrogen is given as $\Delta S$ that equal to 130 kJ/mol K[49] in Equation (2). $Ca_3CH$ has a high hydrogen desorption temperature (1891 K) because of a high formation enthalpy (−2.56 eV/atom) while the hydrogen doping to $Ca_3CH$ decreases the formation enthalpy (−0.72

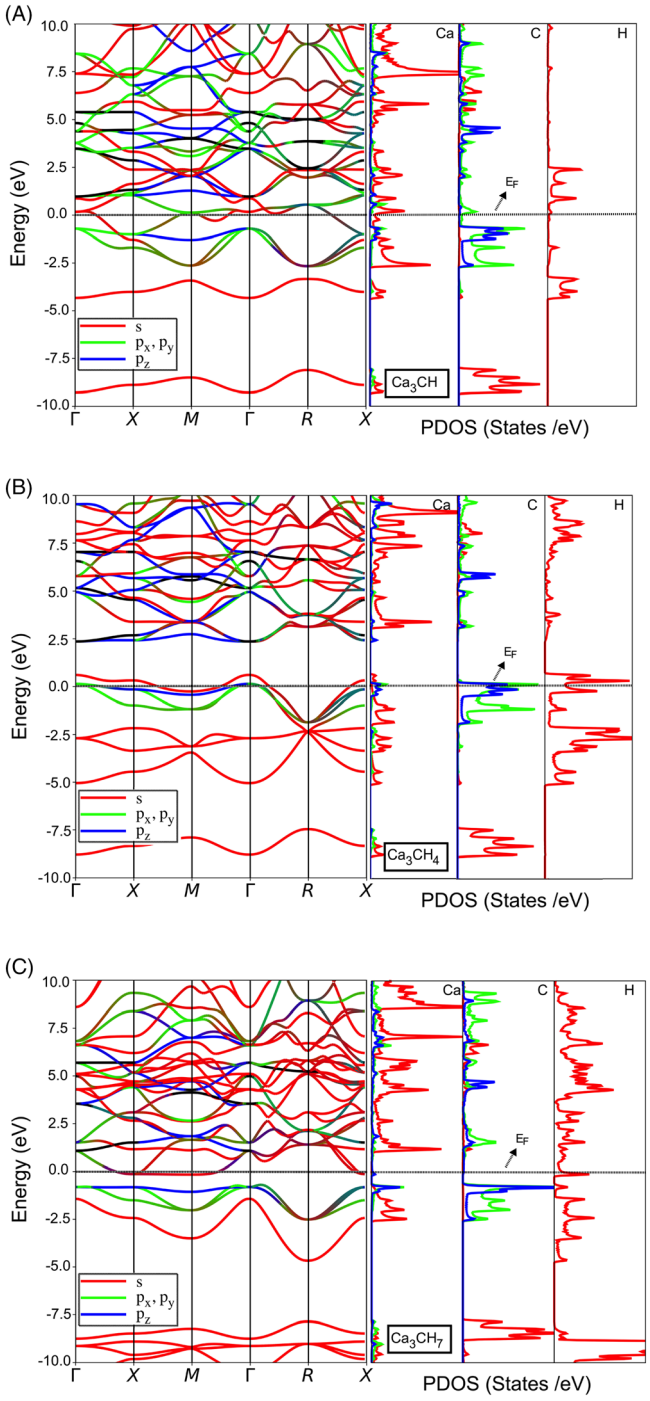


**FIGURE 3** The band structures and corresponding partial density of states (PDOS) for (A) $Ca_3CH$, (B) $Ca_3CH_4$, (C) $Ca_3CH_7$, (D) $Ca_3CH_9$, and (E) $Ca_3CH_{10}$ [Colour figure can be viewed at wileyonlinelibrary.com]

eV/atom) that results lower hydrogen desorption temperatures (534 K). Therefore, the largest capacity belongs to $Ca_3CH_{10}$ and the smallest temperature belongs to $Ca_3CH_9$ among the studied compounds.

$$H = T \times S \tag{2}$$

The band structures have been obtained along the high symmetry points in the first Brillouin zone as well as the partial density of states (PDOS) as shown in Figure 3A-E for $Ca_3CH$, $Ca_3CH_4$, $Ca_3CH_7$, $Ca_3CH_9$, and $Ca_3CH_{10}$, respectively. All compounds have metallic character as can be seen from the figures. In the band structures and the PDOS plots, the colors correspond to the contributions coming from $s$ (red), $p_x$, $p_y$ (green), and $p_z$ (blue) orbitals. More contributions to the PDOS come from $s$ orbitals of H atoms if the compound has more hydrogen atoms in its structure. In addition, if the compound has more hydrogen atoms, the contribution at the Fermi level coming from $s$ orbitals of H atoms increases. For $Ca_3CH$, there is a strong hybridization between the $s$ orbital of Ca atoms and the $p_x$, $p_y$ orbitals of the C atom in −2.8 to 0.8 eV range. $Ca_3CH_4$ has a strong hybridization between the $s$ orbital of H atoms and the $s$ orbital of Ca atoms in −3.0 to −2.0 eV range, and also there is a strong hybridization between the $s$ orbital of Ca atoms and the $p$ orbital ($p_x$, $p_y$, $p_z$) of C atoms in −2.0 to −0.5 eV range. In addition, there is a strong hybridization between the $s$ orbital of H atoms and the $p$ orbitals of C atom at the Fermi level for $Ca_3CH_4$, which results in an electronic unstability tendency of $Ca_3CH_4$. For $Ca_3CH_7$, there is a strong hybridization between the $s$ orbital of Ca atoms and the $p$ orbital ($p_x$, $p_y$, $p_z$) of C atoms in −3.0 to −0.6 eV range. For $Ca_3CH_9$, there is a strong hybridization between Ca and H atoms in −3.0 to −2.0 eV range. Furthermore, the dominant contribution to the antibonding states comes from the Ca atoms for $Ca_3CH$, $Ca_3CH_4$, and $Ca_3CH_7$. The more hydrogen doping to the structure results with the dominant contributions to the antibonding states coming from the Ca and H atoms for $Ca_3CH_9$ and $Ca_3CH_{10}$.

The ratio of the extent of the occupied states ($W_{occ}$) to the extent of the bonding states ($W_b$) could be used to discuss the phase stability of a compound using band filling theory.[50-52] If the $W_{occ}/W_b$ ratio is around 1, the stability of the compound increases. The obtained $W_{occ}/W_b$ ratios are listed in Table 1, and as can be concluded from these ratios, $Ca_3CH$ is the most stable compound where $W_{occ}/W_b$ ratio is 1. Also, the number of electrons at the Fermi level has been listed in Table 1, and the lower value of the number of electrons at the Fermi level indicates the structural stability of these compounds. $Ca_3CH$ has the lowest number of electrons at the Fermi level that implies the structural stability of it while $Ca_3CH_4$ has the highest number of electrons at the Fermi level among $Ca_3CH_x$ compounds implying the less electronic unstability of this compound. Also, the PDOS plot of $Ca_3CH_4$ reveals the hybridization between the $s$ orbital of H atoms and the $p$ orbitals of C atoms at the Fermi level that is the reason of the electronic unstability of this compound.

Figure 4 shows the electron-density distribution for $Ca_3CH_{10}$ in (1 0 0), (1 1 0), and (1 1 1) planes where $Ca_3CH_{10}$ has ionic bonding. The remaining studied compounds have also ionic bonding, and they are not presented here not to keep more space in the journal. Moreover, the charge of each ion in $Ca_3CH_x$ compounds has been obtained with the Bader partial charge analysis as listed in Table 2. The charge transfer could be determined with the sign of the Bader net charge.[13] The atom with a positive Bader charge gives away the charge, and it gets charge with a negative Bader net charge. As can be

**TABLE 2** Bader partial net charges (in electron charge $e$ for per unit cell) for $Ca_3CH$, $Ca_3CH_4$, $Ca_3CH_7$, $Ca_3CH_9$, and $Ca_3CH_{10}$

| Atom | $Ca_3CH$ | $Ca_3CH_4$ | $Ca_3CH_7$ | $Ca_3CH_9$ | $Ca_3CH_{10}$ |
|---|---|---|---|---|---|
| *Ca* | 3.45 | 15.73 | 3.83 | 4.23 | 4.06 |
| *C* | −2.55 | −2.80 | −2.35 | −0.35 | −1.84 |
| *H* | −0.90 | −12.93 | −1.48 | −3.88 | −2.22 |

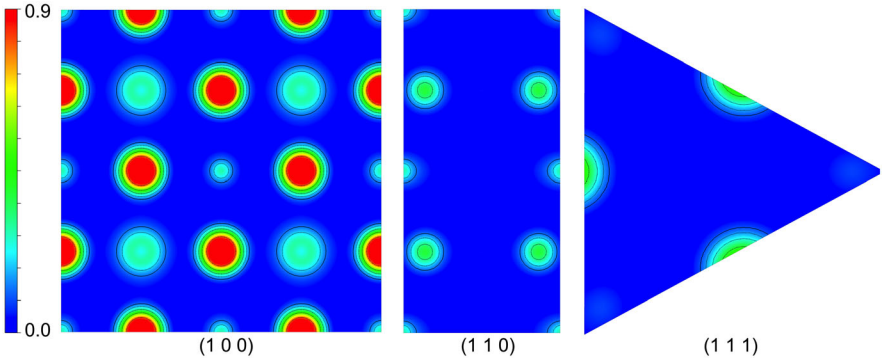


**FIGURE 4** Electron-density distribution for $Ca_3CH_{10}$ in (1 0 0), (1 1 0), and (1 1 1) planes for 2 × 2 × 2 supercell [Colour figure can be viewed at wileyonlinelibrary.com]

concluded from Table 2, the Ca atoms give charge away while the C and H atoms get charge. In addition, each compound has zero total Bader net charge. $Ca_3CH_4$ has higher charges for Ca and H atoms than the remaining compounds that indicates the electronic unstability of this compound consistent with the result of the number of electrons at the Fermi level.

## 4 | CONCLUSION

In this study, $Ca_3CH_x$ ($x$ = 1, 4, 7, 9, and 10) antiperovskite compounds have been investigated using VASP, and it has been found that they are thermodynamically stable and synthesizable. Moreover, when the hydrogen atoms in the compounds increase, the gravimetric storage capacity increases. Also, the desorption temperature decreases with the lower formation enthalpies (−0.72 eV/atom). The calculated band structures show that $Ca_3CH_x$ ($x$ = 1, 7, 9, and 10) compounds show metallic character while $Ca_3CH_4$ is electronically unstable compound among the considered compounds. Also, the Bader partial charge analysis shows that the Ca atoms give charge to the C and H atoms. With the band filling theory, it has been found that $Ca_3CH$ is the electronically most stable compound that is consistent with the result of the formation enthalpy. As known up to date, this is the first consideration of the antiperovskite compounds for hydrogen storage applications and $Ca_3CH_{10}$ compound having 7.10 wt% gravimetric storage capacity and 534.0 K hydrogen desorption temperature is the possible compound with both energetic and electronic stability. This study could lead to the future studies for these compounds.

## ORCID

*Aysenur Gencer* https://orcid.org/0000-0003-2574-3516
*Gokhan Surucu* https://orcid.org/0000-0002-3910-8575

## REFERENCES

1. International Energy Agency. World Energy Outlook 2018. https://www.iea.org/weo2018/ (accessed January 7, 2019).
2. Crabtree GW, Dresselhaus MS, Buchanan MV. The hydrogen economy. *Phys Today*. 2004;57(12):39-44.
3. Niaz S, Manzoor T, Pandith AH. Hydrogen storage: materials, methods and perspectives. *Renew Sustain Energy Rev*. 2015;50:457-469.
4. Abd.Khalim Khafidz NZ, Yaakob Z, Lim KL, Timmiati SN. The kinetics of lightweight solid-state hydrogen storage materials: a review. *Int J Hydrogen Energy*. 2016;41(30):13131-13151.
5. Singh SB, De M. Scope of doped mesoporous (<10 nm) surfactant-modified alumina templated carbons for hydrogen storage applications. *Int J Energy Res*. 2019;43(9):4264-4280.
6. Walker G. (Gavin), Institute of Materials M*Solid State Hydrogen Storage: Materials and Chemistry*. Cambridge: Woodhead Pub.; 2008:600.
7. Kim KC. A review on design strategies for metal hydrides with enhanced reaction thermodynamics for hydrogen storage applications. *Int J Energy Res*. 2018;42(4):1455-1468.
8. Broom DP. *Hydrogen Storage Materials: The Characterisation of Their Storage Properties*. London: Springer; 2011:253.
9. Klechikov AG, Mercier G, Merino P, Blanco S, Merino C, Talyzin AV. Hydrogen storage in bulk graphene-related materials. *Microporous Mesoporous Mater*. 2015;210:46-51.
10. Møller K, Sheppard D, Ravnsbæk D, et al. Complex metal hydrides for hydrogen, thermal and electrochemical energy storage. *Energies*. 2017;10(10):1645.
11. Rusman NAA, Dahari M. A review on the current progress of metal hydrides material for solid-state hydrogen storage applications. *Int J Hydrogen Energy*. 2016;41(28):12108-12126.
12. Yu X, Tang Z, Sun D, Ouyang L, Zhu M. Recent advances and remaining challenges of nanostructured materials for hydrogen storage applications. *Prog Mater Sci*. 2017;88:1-48.
13. Lee SM, Lee YH. Hydrogen storage in single-walled carbon nanotubes. *Appl Phys Lett*. 2000;76(20):2877-2879.
14. Zaluska A, Zaluski L, Ström–Olsen J. Nanocrystalline magnesium for hydrogen storage. *J Alloys Compd*. 1999;288(1-2):217-225.
15. Baysal MB, Surucu G, Deligoz E, Ozısık H. The effect of hydrogen on the electronic, mechanical and phonon properties of $LaMgNi_4$ and its hydrides for hydrogen storage applications. *Int J Hydrogen Energy*. 2018;43(52):23397-23408.
16. Al Alam AF, Matar SF, Ouaïni N, Nakhl M. Hydrogen insertion effects on the magnetic properties and chemical bonding within C14 Laves phases. *Prog Solid State Chem*. 2008;36(3):192-212.
17. Matar SF. Intermetallic hydrides: a review with ab initio aspects. *Prog Solid State Chem*. 2010;38(1-4):1-37.
18. Cobian M, Íñiguez J. Theoretical investigation of hydrogen storage in metal-intercalated graphitic materials. *J Phys Condens Matter*. 2008;20(28):285212.
19. Wolverton C, Siegel DJ, Akbarzadeh AR, Ozoliņš V. Discovery of novel hydrogen storage materials: an atomic scale computational approach. *J Phys Condens Matter*. 2008;20(6):064228.
20. Bonfanti M, Achilli S, Martinazzo R. Sticking of atomic hydrogen on graphene. *J Phys Condens Matter*. 2018;30(28):283002.
21. Milanese C, Jensen TR, Hauback BC, et al. Complex hydrides for energy storage. *Int J Hydrogen Energy*. 2019;44(15):7860-7874.
22. Weidenthaler C. Crystal structure evolution of complex metal aluminum hydrides upon hydrogen release. *J Energy Chem*. 2020;42(2020):133-143.
23. Von Colbe JB, Ares JR, Barale J, et al. Application of hydrides in hydrogen storage and compression: achievements, outlook and perspectives. *Int J Hydrogen Energy*. 2019;44(15):7780-7808.

24. Sathishkumar N, Wu S-Y, Chen H-T. Boron- and nitrogen-doped penta-graphene as a promising material for hydrogen storage: a computational study. *Int J Energy Res.* 2019;43(9):4867-4878.
25. Sakintuna B, Lamari-Darkrim F, Hirscher M. Metal hydride materials for solid hydrogen storage: a review. *Int. J. Hydrogen Energy*. 2007;32(9):1121-1140.
26. Jain IP, Jain P, Jain A. Novel hydrogen storage materials: a review of lightweight complex hydrides. *J. Alloys Compd.* 2010;503(2):303-339.
27. Rehmat B, Rafiq MA, Javed Y, Irshad Z, Ahmed N, Mirza SM. Elastic properties of perovskite-type hydrides $LiBeH_3$ and $NaBeH_3$ for hydrogen storage. *Int J Hydrogen Energy*. 2017;42(15):10038-10046.
28. Benlamari S, Bendjeddou H, Boulechfar R, et al. Structural, electronic, elastic, and thermal properties of $CaNiH_3$ perovskite obtained from first-principles calculations. *Chinese Phys B*. 2018;27(3):037104.
29. Li Y, Mi Y, Chung JS, Kang SG. First-principles studies of $K_{1-x}M_xMgH_3$ (M = Li, Na, Rb, or Cs) perovskite hydrides for hydrogen storage. *Int J Hydrogen Energy*. 2018;43(4):2232-2236.
30. Bouhadda Y, Bououdina M, Fenineche N, Boudouma Y. Elastic properties of perovskite-type hydride $NaMgH_3$ for hydrogen storage. *Int J Hydrogen Energy*. 2013;38(3):1484-1489.
31. Ikeda K, Kogure Y, Nakamori Y, Orimo S. Formation region and hydrogen storage abilities of perovskite-type hydrides. *Prog Solid State Chem*. 2007;35(2-4):329-337.
32. Gencer A, Surucu G. Investigation of structural, electronic and lattice dynamical properties of $XNiH_3$ (X = Li, Na and K) perovskite type hydrides and their hydrogen storage applications. *Int J Hydrogen Energy*. 2019;44(29):15173-15182.
33. Raza HH, Murtaza G, Umm-e-Hani KRMA. Optoelectronic and thermal properties of $LiXH_3$(X = Ba, Sr and Cs) for hydrogen storage materials: a first principle study. *Solid State Commun*. 2019;299:113659.
34. Rkhis M, Alaoui-Belghiti A, Laasri S, et al. First principle investigation on hydrogen solid storage in $Zr_{1-x}Nb_xNiH_3$ ($x$ = 0 and 0.1). *Int J Hydrogen Energy*. 2019;44(41):23188-23195.
35. Wang Z, Tao S, Deng J, Zhou H, Yao Q. Significant improvement in the dehydriding properties of perovskite hydrides, $NaMgH_3$, by doping with $K_2TiF_6$. *Int J Hydrogen Energy*. 2017;42(12):8554-8559.
36. Moure C, Peña O. Recent advances in perovskites: processing and properties. *Prog Solid State Chem*. 2015;43(4):123-148.
37. Gencer A, Surucu G, Al S. $MgTiO_3H_x$ and $CaTiO_3H_x$ perovskite compounds for hydrogen storage applications. *Int J Hydrogen Energy*. 2019;44(23):11930-11938.
38. Gencer A, Surucu G. Density functional theory (DFT) study of $BaScO_3H_{0.5}$ compound and its hydrogen storage properties. *Can J Phys*. 2019; 1-9. https://doi.org/10.1139/cjp-2018-0733
39. Gencer A, Surucu S. Properties of $BaYO_3$ perovskite and hydrogen storage properties of $BaYO_3H_x$. *Int J Hydrogen Energy*. 2019. https://doi.org/10.1016/j.ijhydene.2019.06.198
40. Kresse G, Furthmüller J. Efficient iterative schemes for ab initio total-energy calculations using a plane-wave basis set. *Phys Rev B*. 1996;54(16):11169-11186.
41. Kresse G, Furthmüller J. Efficiency of ab-initio total energy calculations for metals and semiconductors using a plane-wave basis set. *Comput Mater Sci*. 1996;6(1):15-50.
42. Blöchl PE. Projector augmented-wave method. *Phys Rev B*. 1994;50(24):17953-17979.
43. Kresse G, Joubert D. From ultrasoft pseudopotentials to the projector augmented-wave method. *Phys Rev B*. 1999;59(3):1758-1775.
44. Perdew JP, Burke K, Ernzerhof M. Generalized gradient approximation made simple. *Phys Rev Lett*. 1996;77(18):3865-3868.
45. Pack JD, Monkhorst HJ. "Special points for Brillouin-zone integrations"—a reply. *Phys Rev B*. 1977;16(4):1748-1749.
46. Tang W, Sanville E, Henkelman G. A grid-based Bader analysis algorithm without lattice bias. *J Phys Condens Matter*. 2009;21(8):084204.
47. Aroyo MI, Perez-Mato JM, Capillas C, et al. Bilbao crystallographic server: I. Databases and crystallographic computing programs. *Zeitschrift Für Krist—Cryst Mater*. 2006;221:15-27.
48. US Department of Energy. "DOE Technical Targets for Hydrogen Storage Systems for Portable Power Equipment, 2019". https://www.energy.gov/eere/fuelcells/doe-technical-targets-hydrogen-storage-systems-portable-power-equipment.
49. Zeng Q, Su K, Zhang L, Xu Y, Cheng L, Yan X. Evaluation of the thermodynamic data of $CH_3SiCl_3$ based on quantum chemistry calculations. *J Phys Chem Ref Data*. 2006;35(3):1385-1390.
50. Surucu G, Colakoglu K, Deligoz E, Ciftci YO. Structural, electronic and mechanical properties of $W_{1-x}Tc_xB_2$ alloys. *Solid State Commun*. 2013;171:1-4.
51. Xu J-H, Oguchi T, Freeman AJ. Crystal structure, phase stability, and magnetism in $Ni_3V$. *Phys Rev B*. 1987;35(13):6940-6943.
52. Xu J, Freeman AJ. Band filling and structural stability of cubic trialuminides: $YAl_3$, $ZrAl_3$, and $NbAl_3$. *Phys Rev B*. 1989;40(17):11927-11930.


**How to cite this article:** Gencer A, Surucu G. Enhancement of hydrogen storage properties of $Ca_3CH$ antiperovskite compound with hydrogen doping. *Int J Energy Res*. 2020;44:567–573. https://doi.org/10.1002/er.4887